



Original Article

Fast non-local means noise reduction algorithm with acceleration function for improvement of image quality in gamma camera system: A phantom study

Chan Rok Park ^a, Youngjin Lee ^{b,*}

^a Department of Nuclear Medicine, Seoul National University Hospital, 101, Daehak-Ro, Jongno-Gu, Seoul, Republic of Korea

^b Department of Radiological Science, Gachon University, 191, Hambakmoero, Yeonsu-gu, Incheon, Republic of Korea

ARTICLE INFO

Article history:

Received 9 August 2018

Received in revised form

15 November 2018

Accepted 20 December 2018

Available online 21 December 2018

Keywords:

Medical application

Gamma camera system

Noise reduction algorithm

Total variation noise reduction method

Evaluation of image quality

ABSTRACT

Gamma-ray images generally suffer from a lot of noise because of low photon detection in the gamma camera system. The purpose of this study is to improve the image quality in gamma-ray images using a gamma camera system with a fast nonlocal means (FNLM) noise reduction algorithm with an acceleration function. The designed FNLM algorithm is based on local region considerations, including the Euclidean distance in the gamma-ray image and use of the encoded information. To evaluate the noise characteristics, the normalized noise power spectrum (NNPS), contrast-to-noise ratio (CNR), and coefficient of variation (COV) were used. According to the NNPS result, the lowest values can be obtained using the FNLM noise reduction algorithm. In addition, when the conventional methods and the FNLM noise reduction algorithm were compared, the average CNR and COV using the proposed algorithm were approximately 2.23 and 7.95 times better than those of the noisy image, respectively. In particular, the image-processing time of the FNLM noise reduction algorithm can achieve the fastest time compared with conventional noise reduction methods. The results of the image qualities related to noise characteristics demonstrated the superiority of the proposed FNLM noise reduction algorithm in a gamma camera system.

© 2018 Korean Nuclear Society, Published by Elsevier Korea LLC. This is an open access article under the CC BY-NC-ND license (<http://creativecommons.org/licenses/by-nc-nd/4.0/>).

1. Introduction

Nuclear medicine imaging techniques, including gamma cameras and single-photon emission computed tomography (SPECT), are crucial applications in the field of medical diagnosis and therapy [1–4]. In gamma cameras and SPECT, the collimator can focus the gamma ray onto the detector and can localize the gamma-ray source in the patient [5,6].

However, the gamma camera or SPECT system using gamma rays is an inherently noisy investigation [7]. Many noises impair and diminish the detectability of a target region in an image, especially if it is a low-contrast object. In gamma-ray images, noise consists of two types: (1) structured noise with nonrandom count density and (2) random noise with statistical or quantum mottle.

To reduce noise in gamma-ray images, noise reduction

algorithms have been developed by researchers [8,9]. Among these algorithms, median and Wiener filters are used as the default method in the field of medical imaging [10,11]. A median filter is widely used, because it is effective for noise reduction, calculating by first sorting all the pixel values, and the Wiener filter is based on a stationary linear filter using the frequency domain (discrete Fourier transform) for images degraded by noise. However, the one major drawback of median and Wiener filters is a lack of edge information preservation. To address this problem, a noise reduction algorithm with a total variation (TV) approach was introduced by Rudin et al., [12]. A TV noise reduction algorithm is a computationally efficient filtering method with the signal changes between signal values using an iterative process [12–14]. There is now extensive research that shows the effectiveness of the above-mentioned noise reduction algorithms in medical images. In this study, a fast nonlocal means (FNLM)-based noise reduction algorithm was designed using an acceleration function. There have been many studies on the FNLM noise reduction algorithm in X-ray imaging systems, but few on quantitative evaluations of gamma-ray imaging systems for creating the algorithm-applied images.

* Corresponding author. Department of Radiological Science, Gachon University, 191, Hambakmoero, Yeonsu-gu, Incheon, Republic of Korea.
E-mail address: yj20@gachon.ac.kr (Y. Lee).

Therefore, the purpose of this work was to evaluate image performance related to the noise characteristics using the proposed FNLM noise reduction algorithm (compared with the median filter, Wiener filter, and TV noise reduction algorithm) in a gamma camera system using a low-energy, high-resolution parallel-hole collimator. The normalized noise power spectrum (NNPS), contrast-to-noise ratio (CNR), and coefficient of variation (COV) for the algorithm were evaluated in an experimental gamma-ray image.

2. Materials and methods

2.1. Gamma-ray image acquisition

A gamma camera system (Discovery NM/CT 670, GE Healthcare) was used to acquire gamma-ray images. The low-energy, high-resolution parallel-hole collimator was used, because a ^{99m}Tc source with 140-keV energy was used in this study, and the source-to-collimator distance was 21.0 cm. The phantom used (Flangeless Deluxe Jaszczak) consisted of two main parts: (1) cold sphere regions and (2) cold rod regions. Fig. 1 shows the overall established gamma camera system.

2.2. FNLM noise reduction algorithm design

Before designing the FNLM-based method, the simple nonlocal means (NLM) noise reduction algorithm is defined as follows [15]:

$$\text{NLM}[u_{\text{true}}](x) = \frac{1}{C(x)} \int_{\Omega} e^{-\frac{(G_k * |u_{\text{true}}(x) - u_{\text{true}}(y)|^2)(0)}{h^2}} u_{\text{true}}(y) dy \quad (1)$$

where $x \in \Omega$ is bounded and open set,

$C(x) = \int_{\Omega} e^{-\frac{(G_k * |u_{\text{true}}(x) - u_{\text{true}}(z)|^2)(0)}{h^2}} dz$ is the normalization constant, G_k is the Gaussian kernel, and h is the filtering parameter. The biggest difference between the NLM noise reduction algorithm and conventional filters (local or frequency domain filters) is the systemic utilization with self-predictions in the image [16].

However, one of the concerns with using the NLM noise reduction algorithm is the low time resolution in image processing. To address the low time resolution problem, the acceleration function was used with Euclidean distance based on comparing two

neighborhood pixels with the fast Fourier transform and summed squared image [17].

$$\begin{aligned} S(i, j) &= \|N_i - N_j\|_{j a_k}^2 = \sum_{l=0}^{M-1} \sum_{m=0}^{M-1} [I_i(l, m) - I_j(l - x'_j, m - y'_j)]^2 \\ &= N_i^2 + N_j^2 - N_i * N_j \end{aligned} \quad (2)$$

where $S(i, j)$ is estimated by the Euclidean distance of neighborhood pixels N_i and N_j with window size (M, M) , a_k is the standard deviation of the Gaussian kernel, and $I_i(l, m)$ and $I_j(l, m)$ are the corresponding in N_i and N_j , respectively.

To compare the image performances of the noise reduction algorithms, conventional methods using the median filter, Wiener filter, and TV noise reduction algorithm were also used.

2.3. Evaluation of image performances

To evaluate the capability of the FNLM noise reduction algorithm for the gamma camera system, the NNPS, CNR, and COV were calculated as follows:

$$\begin{aligned} \text{NNPS}(u, v) &= \frac{\text{NPS}(u, v)}{(\text{mean signal of average ROI})^2} \\ \text{NPS}(u_n, v_k) &= \lim_{N_x, N_y \rightarrow \infty} (N_x N_y \Delta x \Delta y) < |\text{FT}_{\text{nk}} I(x, y) - S(x, y)|^2 > \\ &= \lim_{N_x, N_y \rightarrow \infty} \lim_{M \rightarrow \infty} \frac{(N_x N_y \Delta x \Delta y)}{M} \sum_{m=1}^M |\text{FT}_{\text{nk}} I(x, y) - S(x, y)|^2 \\ &= \lim_{N_x, N_y, M \rightarrow \infty} \frac{\Delta x \Delta y}{M \cdot N_x N_y} \sum_{m=1}^M \left| \sum_{j=1}^{N_x} \sum_{l=1}^{N_y} (I(x_j, y_l) - S(x, y)) \exp(-2\pi i(u_n x_j + v_k y_l)) \right|^2 \end{aligned} \quad (3)$$

where u and v are the spatial frequency conjugates in the X and Y directions, respectively; N_x and N_y are the number of pixels in the X and Y directions, respectively (e.g., N_x and N_y are both 64 pixels in this study); Δx and Δy are the pixel spacing in the X and Y directions, respectively (e.g., Δx and Δy are both 3 mm in this study); $I(x_j, y_l)$ is the image intensity at the (x_j, y_l) pixel location; $S(x, y)$ is the mean intensity; M is the number of ensemble averages and we implemented the radial averaging at four groups of 16 X 16 pixels. Here, it is necessary to balance between the best possible value of the region of interest (ROI) size and M for certainty in the estimate of NPS. For the details of the NPS, can be found in Refs. [18,19].

$$\text{CNR} = \frac{|O_T - O_B|}{\sqrt{\sigma_T^2 + \sigma_B^2}} \quad (4)$$

$$\text{COV} = \frac{\sigma_T}{O_T} \quad (5)$$

where O_T and σ_T are the mean and the standard deviation for the target ROI, respectively; and O_B and σ_B are the mean and the standard deviation for the background ROI, respectively.

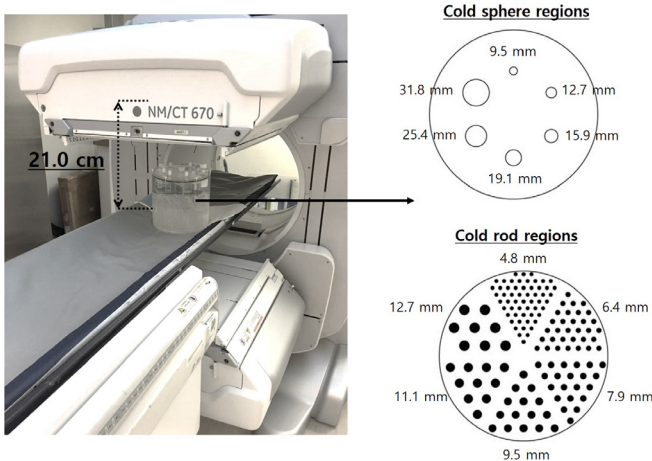


Fig. 1. Photo of the gamma camera system (six areas with spheres were located in a phantom: 9.5, 12.7, 15.9, 19.1, 25.4, and 31.8 mm diameters; six areas with rods were located in a phantom: 4.8, 6.4, 7.9, 9.5, 11.1, and 12.7 mm diameters).

3. Results and discussion

The feasibility of the FNLM noise reduction algorithm in Deluxe Jaszczak phantom images with the gamma camera system was confirmed. Figs. 2 and 3 show the acquired phantom image with different noise reduction methods, including the FNLM algorithm using cold sphere regions and cold rod regions, respectively.

The calculated NNPS result using the conventional noise reduction methods and the proposed FNLM noise reduction algorithm is shown in Fig. 4. The NNPS result of the TV noise reduction algorithm can acquire the lowest value (approximately 10^{-8} mm^2 in both the cold sphere phantom and the cold rod phantom) and is 10 to 10^2 times ($\sim 1.5 \text{ mm}^{-1}$ spatial frequency) and 10^2 to 10^5 times ($\sim 1.5 \text{ mm}^{-1}$ spatial frequency) lower than that of the median or Wiener filter. It was proved that the proposed FNLM noise reduction algorithm can effectively eliminate the noise intensity by a much greater degree in the cold region phantom using the gamma camera system and achieve improved noise characteristics. In addition, the result confirmed that the calculated NNPS values decreased sharply with the spatial frequency at approximately 1.5 mm^{-1} in the gamma camera system.

The evaluated CNR and COV results using conventional noise reduction methods and the proposed FNLM noise reduction algorithm in the gamma camera system is shown in Fig. 5. In the cold sphere and rod phantoms, the evaluated CNR increases from the median filter to the Wiener filter, via the TV noise reduction algorithm, to the proposed FNLM noise reduction algorithm in that order. In the cold sphere phantom, when the conventional methods and the FNLM noise reduction algorithm were compared, the CNR using the proposed algorithm was approximately 2.27, 1.46, 1.35, and 1.29 times higher than those of the noisy image, median filter, Wiener filter, and TV noise reduction algorithms, respectively. In the cold rod phantom, when the conventional methods and the FNLM noise reduction algorithm were compared, the CNR using the proposed algorithm was approximately 2.21, 1.41, 1.31, and 1.26 times higher than those of the noisy image, median filter, Wiener filter, and TV noise reduction algorithms, respectively.

In addition, the evaluated COV goes from the proposed FNLM noise reduction algorithm to the TV noise reduction algorithm, via the Wiener filter, to the median filter, in increasing order, in the cold sphere and rod phantoms. In the cold sphere phantom, when the conventional methods and the FNLM noise reduction algorithm

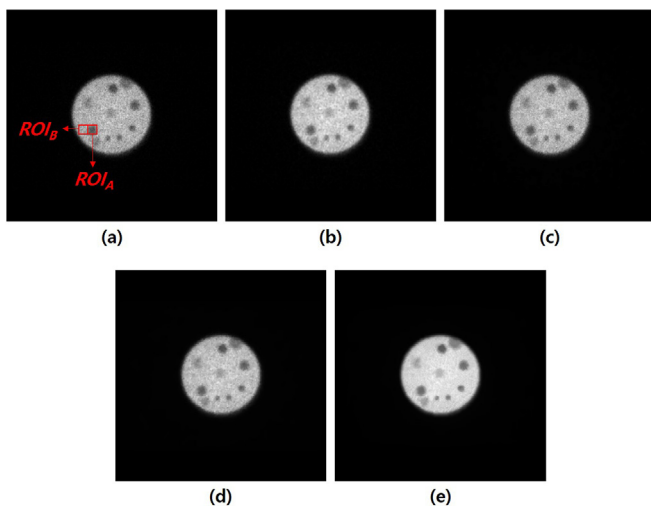


Fig. 2. Result phantom images using cold sphere regions for the (a) noisy including ROIs (NNPS calculation: ROI_B; CNR calculation: ROI_A and ROI_B; and COV calculation: ROI_A), (b) median filter, (c) Wiener filter, (d) TV noise reduction algorithm, and (e) FNLM noise reduction algorithm in gamma camera system.

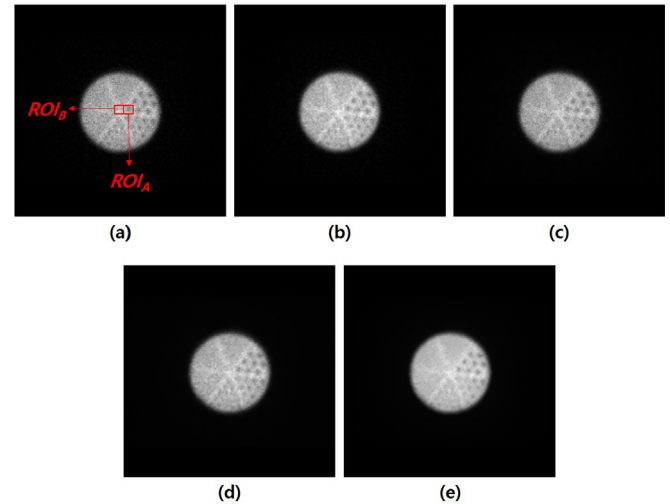


Fig. 3. Result phantom images using cold rod regions for the (a) noisy including ROIs (NNPS calculation: ROI_B; CNR calculation: ROI_A and ROI_B; and COV calculation: ROI_A), (b) median filter, (c) Wiener filter, (d) TV noise reduction algorithm, and (e) FNLM noise reduction algorithm in gamma camera system.

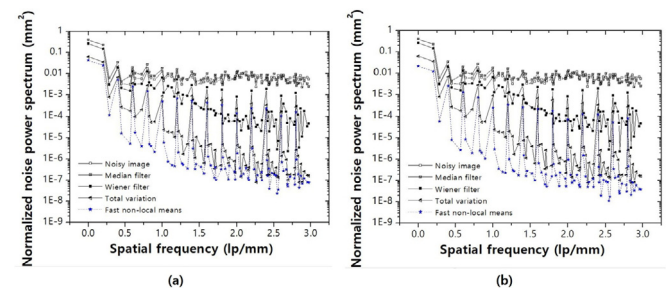


Fig. 4. NNPS results for the different noise reduction methods in (a) cold sphere phantom and (b) cold rod phantom.

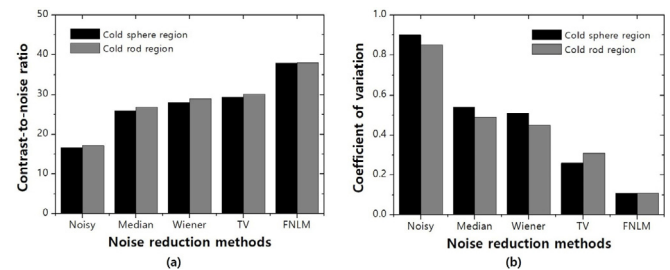


Fig. 5. (a) CNR and (b) COV results for each noise reduction method in cold sphere and cold rod phantoms.

were compared, the COV using the proposed algorithm was approximately 8.18, 4.91, 4.64, and 2.36 times better than those of the noisy image, median filter, Wiener filter, and TV noise reduction algorithms, respectively. In the cold rod phantom, when the conventional methods and the FNLM noise reduction algorithm were compared, the COV using the proposed algorithm was approximately 7.73, 4.45, 4.09, and 2.82 times better than those of the noisy image, median filter, Wiener filter, and TV noise reduction algorithms, respectively.

In particular, the temporal resolution can be improved because of the term of the acceleration function considering the Euclidean distance in the designed algorithm. The time required to denoise the phantom image in the gamma camera system was calculated

for each noise reduction method, with the fastest being the FNLN algorithm in all phantom images. The computer system used for the experiments was an Intel dual core CPU (Q9550 2.8 GHz) and NVIDIA GeForce graphic card (9500 GS). The average processing time was approximately 0.11 s with the proposed FNLN noise reduction algorithm in the acquired cold sphere and rod phantom images (TV noise reduction algorithm, 3.01 s in the same conditions). This processing time is a reasonable duration for a noise reduction algorithm in a gamma camera system.

4. Conclusion

We performed experiments to demonstrate the efficiency of noise reduction with the FNLN noise reduction algorithm in the gamma camera system. In particular, the comparison between the proposed reduction algorithm and the conventional methods was not implemented, since the purpose of this research is to cope with the various problems using image-processing. The results confirmed that the proposed FNLN noise reduction algorithm produced appropriate image quality with acceptable image-processing time.

Acknowledgments

This research was supported by the National Research

Foundation of Korea (NRF-2016R1D1A1B03930357).

References

- [1] E.G. DePuey, J. Nucl. Cardiol. 19 (2012) 1085.
- [2] H.C. Kim, H.J. Kim, K. Kim, M.H. Lee, Y. Lee, Nucl. Eng. Technol. 49 (2017) 776.
- [3] C. Scheiber, Nucl. Instrum. Methods Phys. Res. 448 (2000) 513.
- [4] F.J. Beekman, B. Vastenhout, Phys. Med. Biol. 49 (2004) 4579.
- [5] H.O. Anger, J. Nucl. Med. 5 (1964) 515.
- [6] Y. Lee, H.J. Kim, Nucl. Instrum. Methods Phys. Res. 794 (2015) 54.
- [7] O. Gal, B. Dessus, F. Jean, F. Laine, C. Leveque, IEEE Trans. Nucl. Sci. 48 (2001) 1198.
- [8] S.H. Kim, K. Seo, S.H. kang, S. Bae, H.J. Kwak, J.W. Hong, Y. Hwang, S.M. Kang, H.R. Choi, G.Y. Kim, Y. Lee, J. Magnetics 22 (2017) 570.
- [9] P. Chatterjee, P. Milanfar, IEEE Trans. Nucl. Sci. 19 (2010) 895.
- [10] E. Arias-Castro, D.L. Donoho, Ann. Stat. 37 (2009) 1172.
- [11] X. Zhang, Optik 127 (2016) 6821.
- [12] L.I. Rudin, S. Osher, E. Fatemi, Physica D 60 (1992) 259.
- [13] Y.M. Huang, M.K. Ng, Y.W. Wen, SIAM J. Imag. Sci. 2 (2009) 20.
- [14] K. Seo, S.H. Kim, S.H. Kang, J. Park, C.L. Lee, Y. Lee, J. Magnetics 21 (2016) 593.
- [15] A. Buades, B. Coll, J.-M. Morel, A non-local algorithm for image denoising, in: IEEE Computer Society Conference on Computer Vision and Pattern Recognition, 2015, <https://doi.org/10.1109/CVPR.2005.38>.
- [16] A. Efros, T. Leung, in: Proceeding of IEEE International Conference on Computer Vision, vol. 2, 1999, p. 1033.
- [17] J. Wang, Y. Guo, Y. Ying, Y. Liu, Q. Peng, Fast non-local algorithm for image denoising, in: IEEE International Conference on Image Processing, 2006, <https://doi.org/10.1109/ICIP.2006.312698>.
- [18] J.T. Dobbins III, D.L. Ergun, L. Rutz, D.A. Hinshaw, H. Blume, D.C. Clark, Med. Phys. 22 (1995) 1581.
- [19] J.T. Dobbins III, E. Samei, N.T. Ranger, Y. Chen, Med. Phys. 33 (2006) 1466.